Review

Research Progress and Key Technical Barriers in CaO/Ca(OH)$_2$ Based Energy Storage: A Systematic Review

Jingxiao Wang [1], Yishi Gu [1], Dingxuan Yuan [1], Zhongjie Shen [1,*], Feng Lv [2], Dayang Wan [3], Yongchuan Gao [3], Yuezhang Duan [3], Qifeng Liang [1], Zhenghua Dai [1] and Haifeng Liu [1,4,†]

[1] National Energy Coal Gasification Technology Research and Development Center and Shanghai Engineering Research Center of Coal Gasification, East China University of Science and Technology, P.O. Box 272, Shanghai 200237, China; y10210113@mail.ecust.edu.cn (J.W.); y82210024@mail.ecust.edu.cn (Y.G.); Y30231066@mail.ecust.edu.cn (D.Y.); qfliang@ecust.edu.cn (Q.L.); chinadai@ecust.edu.cn (Z.D.); hfliu@ecust.edu.cn (H.L.)

[2] RUICHEN PETROCHEMICAL, Shanghai 200233, China; lvfeng@ruichang.com.cn (F.L.)

[3] Luoyang Ruichang Environmental Engineering Co., Ltd., Luoyang 471027, China; wandy@ruichang.com.cn (D.W.); gaoyc@ruichang.com.cn (Y.G.); duanyz@ruichang.com.cn (Y.D.)

[4] Liaoning Petrochemical University, Fushun 113001, China

* Corresponding author. E-mail: zjshen@ecust.edu.cn (Z.S.); Tel.: +86-21-64253933 (Z.S.)

† This author's first affiliation is Liaoning Petrochemical University.

ABSTRACT: The CaO/Ca(OH)$_2$ thermochemical energy storage system has garnered significant attention due to its cost-effectiveness, abundant raw material availability, optimal decomposition thermodynamics, high energy density, and recyclability as a promising candidate for large-scale renewable energy integration. Significant progress has been made in the research field of the CaO/Ca(OH)$_2$ energy storage system, while there are still key issues that require further investigation. This comprehensive review summarizes recent advancements in CaO/Ca(OH)$_2$ thermochemical energy storage systems, focusing on reaction mechanism and optimization through material engineering strategies, thermal-fluid dynamics in reactor configurations, cyclic degradation mechanisms under operational stresses, and scalability constraints in system integration. Persistent technical bottlenecks requiring resolution are discussed, particularly sintering-induced capacity decay and suboptimal heat transfer efficiency. The reactor design and optimization with advanced material modification techniques targeting enhanced stability are introduced as well. These discussions and derived suggestions provide a potential opportunity to bridge fundamental material science discoveries with engineering implementation for enabling deployment in stable utilization of renewable energy.

Keywords: CaO/Ca(OH)$_2$ energy storage system; Reactivity; Heat and mass transfer characteristics; Cyclic stability; Reactor and modification

1. Introduction

Since the turn of the century, rapid advancements in global science and technology, combined with rising material demands, have fueled a significant surge in energy consumption worldwide. Currently, the combustion of fossil fuels still dominates energy consumption. However, the extensive use of fossil fuels faces potential shortages and severe environmental challenges, which has led to a sustained high level of global attention to renewable energy over the past decade [1]. Renewable energy sources, including wind, solar, geothermal, and hydro energy, play a significant role in reducing carbon emissions. Their intermittent supply, grid instability, and unpredictable generation patterns pose persistent challenges to large-scale integration into energy systems [2]. Energy storage systems provide a robust solution to these issues, with thermal energy storage as a prominent research focus in recent years, demonstrating compatibility with wind/solar power systems and industrial waste heat recovery [3].

Solar energy, while a cornerstone of renewables, faces inherent challenges of intermittency, supply discontinuity, and seasonal variability. However, the strategic implementation of energy storage systems bridged the temporal and

spatial gaps between power generation and utilization, thereby ensuring a stable and reliable energy supply. In addition to conventional battery-based energy storage systems, thermal energy storage technologies are broadly classified into three primary categories: sensible heat storage, latent heat storage (phase change), and thermochemical energy storage (TCES) [4–6]. Among these, thermochemical energy storage, as a significant avenue for thermal energy storage, stores energy in the form of chemical energy through the endothermic decomposition of materials and releases energy through the reversible exothermic synthesis reactions when required [6]. Thermochemical energy storage technologies are typically classified into three categories based on their operating temperature ranges: low-temperature (<150 °C), medium-temperature (150–400 °C), and high-temperature (>400 °C) systems, with calcium-based systems emerging as a promising candidate for medium-to-high temperature applications [7]. The CaO/Ca(OH)$_2$ thermochemical energy storage system exhibits long-term stability at ambient temperatures while demonstrating a high volumetric energy density [3].

The CaO/Ca(OH)$_2$ system, as a representative gas-solid thermochemical energy storage system, emerges for medium-high temperature applications (200–500 °C) due to its remarkable economic viability, inherent safety profile, and environmental compatibility [8]. Recent advancements further validate its technical feasibility in solar thermal storage integration and the cascading utilization of industrial waste heat, particularly in the decarbonization of cement production and calcium-looping power cycles [9]. The CaO/Ca(OH)$_2$ energy storage system absorbs and generates heat through dehydration and hydration reactions. The process generally comprises two stages: during the endothermic phase, heat is extracted from the CSP plant to decompose Ca(OH)$_2$ into CaO and H$_2$O, with the resulting products being stored separately. During the exothermic phase, the previously stored products are utilized for the next round of reactions. At night, chemical energy is converted into thermal energy through hydration, and the released heat reduces coal consumption, ensuring the normal operation of the CSP plant [10].

Fundamental research focusing on reaction kinetics revealed that in the 400 to 560 °C temperature range and at partial steam pressures from 0 to 100 kPa, the CaO particles react following a chemically controlled first order reaction, displaying activation energies of 59.4 kJ/mol and 60.8 kJ/mol and pre-exponential factors of 2.5×10^{-6} 1/s and 5.2×10^{2} 1/s (for a particle size of 100–200 μm) for hydration and dehydration reactions, respectively [11]. The reaction temperature was a key factor in controlling the direction of reversible Ca-based thermochemical energy storage reactions. The dehydration of calcium hydroxide began at 400 °C, with the desorption rate significantly accelerating above 500 °C, while the hydration reaction of calcium oxide was suppressed or halted when the temperature approached or exceeded 400 °C [12]. Researchers also found that CaO/Ca(OH)$_2$ exhibited excellent cyclic stability—maintaining a 95% hydration degree after 211 cycles—but experienced a decline in reaction rate and Ca(OH)$_2$ agglomeration, which prevented uniform reaction and heat-transfer fluid distribution in the fixed-bed reactor [13,14]. The material modification indicated that compared to the pellets composed entirely of pure Ca(OH)$_2$, the structurally modified TiO$_2$-CaO-based pellets exhibited significantly better heat storage/release performance during the cycling process. After 20 cycles, their performance was nearly 1.3 times that of the pure Ca(OH)$_2$ pellets [15]. Theoretically, smaller particles were less prone to fragmentation, and their larger specific surface area enhanced heat and mass transfer interactions with the reactive fluid. However, continuously reducing particle size was not always feasible. When the particle size diminished to the nanoscale, particle agglomeration driven by van der Waals forces and other interactions became significantly more pronounced, while the demands for steam management also intensified [16].

In recent years, several scholars have conducted comprehensive reviews of thermochemical energy storage based on CaO/Ca(OH)$_2$. Yuan et al. [17] systematically examined the CaO/CaCO$_3$ cycle, the CaO/Ca(OH)$_2$ cycle, and their coupling, demonstrating that high dehydroxylation temperatures, low initial hydration temperatures, elevated water vapor pressures, and the use of circulating fluidized beds markedly enhance storage performance; they further showed that additives such as Al$_2$O$_3$, Na$_2$Si$_3$O$_7$, and nanoscale SiO$_2$ improve structural stability, while LiOH doping boosts material reactivity. Boning [18] provided a thorough analysis of the structural, thermodynamic, and kinetic aspects of the CaO/Ca(OH)$_2$ reactions, revealing that the cubic-to-hexagonal phase transition during hydration induces volumetric expansion and crack formation that facilitates diffusion; they evaluated specific heat capacities, reaction enthalpies, and the effects of temperature, particle size, and material ratios on reaction rates, and discussed the role of γ-Al$_2$O$_3$ and similar enhancers in preventing agglomeration and improving efficiency. Wang et al. [3] focused on the practical implementation of Ca(OH)$_2$/CaO systems in thermochemical storage devices, detailing various reactor designs (including ceramic honeycomb supports, porous ceramic composites, and particle coating techniques), cycle stability, and exothermic behavior under fluidized-bed conditions, thereby providing comprehensive guidance for engineering applications.

In this article, we systematically examined the recent advances in CaO/Ca(OH)$_2$-based thermochemical energy storage systems, with particular emphasis on fundamental mechanisms and performance enhancement strategies. Key aspects analyzed included the reaction thermodynamics and kinetics, with particular attention to the hysteresis behavior

observed in hydration and dehydration cycles and its dependence on the partial pressure of water vapor. Material engineering approaches to mitigate sintering, including nanostructuring, porous matrix stabilization, and surface functionalization to accelerate ion diffusion, were discussed. Reactor-level thermal-fluid synergies, encompassing reactor configurations with quantified heat transfer coefficients and the optimization of residence time, were also included in this review. Cyclic stability and sintering kinetics, which are crucial to the reaction and heat transfer, were summarized, highlighting that operating stresses, both thermal and mechanical, reduced effective capacity due to pore collapse and active site deactivation. Finally, techno-economic barriers to commercial deployment were discussed, with hybrid systems coupling thermochemical energy storage with latent heat storage proposed as a transitional strategy.

2. Reactivity of Ca(OH)$_2$/CaO Cycle

2.1. Dehydration Reaction

The thermal decomposition and dehydration of calcium hydroxide represent a complex multi-scale physicochemical process. This reaction involves interrelated phenomena spanning atomic, nano- and microcrystalline, and macroscopic scales, each demanding distinct theoretical frameworks for analysis [17].

At the atomic and electronic scales, researchers focused on the chemical reaction dynamics. The process begins with the breaking of chemical bonds in calcium hydroxide and the subsequent formation of calcium oxide and water vapor. Quantum mechanical calculations and molecular dynamics simulations are employed to investigate the electronic interactions and interface kinetics that govern bond dissociation and the nucleation of the solid product, calcium oxide [19–22]. These models reveal how localized energy barriers and atomic rearrangements influence reaction rates, offering insights into the fundamental mechanisms driving the dehydration process [21]. Although gas-solid reaction systems exhibit different types of reactions depending on the reactants involved, the underlying microscopic physical and chemical steps are similar. For porous Ca(OH)$_2$ particles, Ca(OH)$_2$ undergoes thermal decomposition, and the generated water molecules diffuse through the pores from the interior to the exterior of the particles, as illustrated in Figure 1 [23].
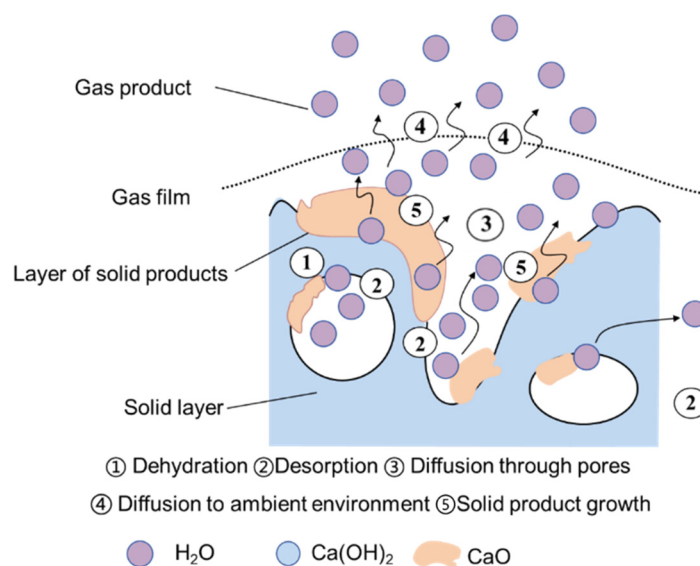

Figure 1. Schematical diagram of dehydration of Ca(OH)$_2$, modified from Ref. [23].

At the nano- and microcrystalline levels, diffusion through the reactant or product layer becomes particularly significant. As the reaction progressed, a porous CaO layer formed, providing channels through which water molecules and ions diffused. The thermal decomposition of calcium hydroxide is a dynamic process, with new layers of solid products continuously growing within the calcium hydroxide particles [20]. There is also a noticeable difference in the molar volumes between the solid products and the solid reactants. Consequently, the growth of solid products alters the pore structure of the particles, affecting the diffusion resistance encountered by water vapor as it enters the calcium hydroxide particles. As a result, the growth of solid products during the reaction leads to changes in the reaction's controlling step. At the initial stage of the reaction, the calcium hydroxide particles, being naturally porous, have relatively large internal pore sizes, resulting in lower mass transfer resistance for water vapor entering the particles. At this stage, the surface chemical reaction at the reaction interface was the rate-determining step [24]. If the volume of the solid products generated during the reaction is greater than that of the solid reactants consumed, the solid products

gradually replace the reactants inside the particles, leading to a reduction in internal pore size or even blockage of the particle pores. As a result, internal gas diffusion eventually replaces the surface chemical reaction as the new rate-determining step [25].

Fickian diffusion models and Monte Carlo simulations were applied to analyze ion transport through the evolving microstructure [26]. The porosity and crystallinity of the CaO layer significantly affected diffusion coefficients, necessitating mesoscale models that bridged atomic interactions with continuum properties. Challenges included predicting how microstructural evolution, such as pore coarsening or sintering, impacted overall reaction kinetics [27]. By studying the dehydration reaction kinetics of calcium hydroxide, the activation energy and pre-exponential factor could be determined, providing insight into the overall reaction rate and the appropriate reaction temperature for the dehydration process.

The physicochemical processes in the TCES system are typically multiscale, involving both reactor-scale and particle-scale dynamics, as shown in Figure 2 [28]. At the reactor scale, where macroscopic transport phenomena dominate, the focus of investigation shifts to the external diffusion of water vapor, both away from the particle surfaces and through the surrounding gas bulk. Here, computational fluid dynamics (CFD) is employed to simulate convective and diffusive transport within reactor environments [29]. Particle size distributions, bed morphology, and gas flow dynamics become critical factors, necessitating the use of empirical correlations such as the Sherwood number to describe mass transfer coefficients [30]. The results are pivotal for industrial reactor design, where optimizing heat and mass transfer enhances overall process efficiency.
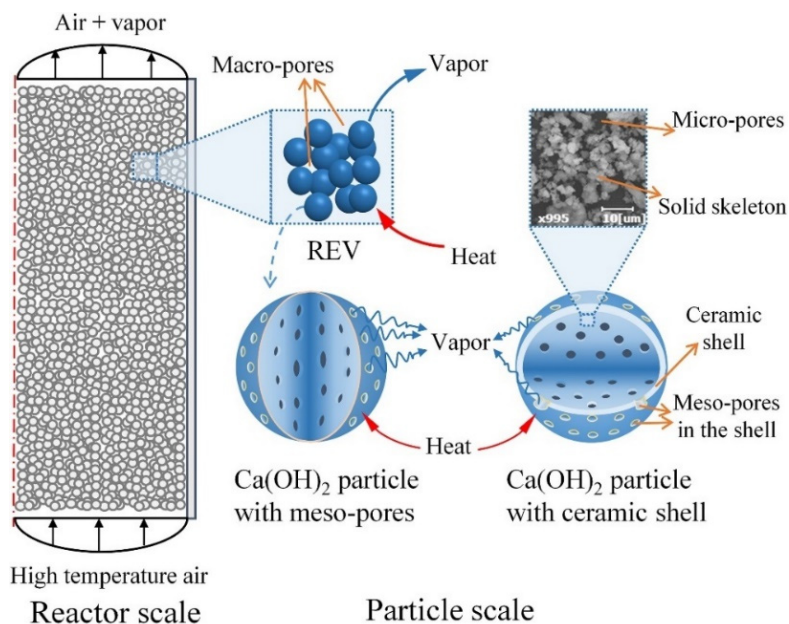

Figure 2. Schematic of the multiscale structures and the multiscale Ca(OH)$_2$ dehydration process, modified from Ref. [28].

The study of the dehydration kinetics of Ca(OH)$_2$ is a particularly important step in understanding and mastering the chemical reaction process of the CaO/Ca(OH)$_2$ energy storage system. Through thermal analysis methods, the micro-mechanism after the reaction, the reaction kinetic parameters, and the thermodynamic control equations could be determined, enabling prediction of the entire chemical energy storage process [14]. The dehydrothermal decomposition process of Ca(OH)$_2$:

$$Ca(OH)_2(s) \rightleftharpoons CaO(s) + H_2O(g), \quad \Delta H = 104 \text{ kJ/mol} \tag{1}$$
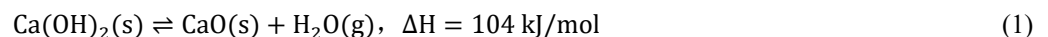
Consider the effect of the rate of warming γ in conjunction with the Arrhenius equation:

$$\frac{d\alpha}{dt} = \left(\frac{A}{\gamma}\right) \cdot exp\left(-\frac{E}{RT}\right) \cdot f(\alpha) \tag{2}$$

where, γ is the rate of temperature increase (K/min); t is the reaction time (s); A denotes the pre-exponential factor (1/s); E is the activation energy of the reaction (J/mol); R is the ideal gas constant, 8.314 J/(mol·K); $f(\alpha)$ denotes the kinetic mechanism function suitable for the thermal decomposition process of calcium hydroxide as shown in Table 1; and α denotes the rate of conversion, which is based on the thermogravimetric experimental considerations:

$$a = (m_i - m_t)/(m_i - m_f) \tag{3}$$

where m_i, m_t and m_f denote the initial mass of the calcium hydroxide sample, the sample mass at time *t*, and the final sample mass, respectively [31].

Table 1. Reaction mechanism functions suitable for $Ca(OH)_2$ dehydration kinetics [32].

Function Name	$f(\alpha)$
The Jander equation	$4(1-\alpha)^{1/2}[1-(1-\alpha)^{1/2}]^{1/2}$
The Jander equation	$6(1-\alpha)^{2/3}[1-(1-\alpha)^{1/3}]^{1/2}$
The reaction order	$4(1-\alpha)^{3/4}$
Contraction ball (volume)	$3(1-\alpha)^{2/3}$
Contraction cylinder (area)	$2(1-\alpha)^{1/2}$

The dehydration kinetics of calcium hydroxide are modeled using reaction mechanisms that account for nucleation, diffusion, and interface processes, which are given in Table 2.

Table 2. Kinetic modelling of $Ca(OH)_2$ dehydration reactions.

Gas	Reaction Kinetics Modeling	References
Air	$-\dfrac{d\omega}{dt} = k(T) \cdot f(\omega)$	Mikhail [33]
	$\dfrac{\ln[P/(P-PA)]}{T_0 - T_c} = \dfrac{ke}{CD_e A(-\Delta HA)}$	Dutta [34]
	$\dfrac{dXD_{ehy}}{dt} = kD_{ehy}(T)(v_{eq} - v_{H_2O})f(XD_{ehy})$	Criado [11]
Vacuum	$ade = \dfrac{74mH_2O}{18mCa(OH)_2} \times 100\%$	Yan [12]
	$\dfrac{d\alpha}{dt} = k[Ca(OH)_2][P_{H_2O}]^{0.5}$	Chaix-Pluchery [35]
Nitrogen	$E = 96.03 – 107.32\,\text{kJ/mol}, A = 1.70 \times 10^5 – 1.23 \times 10^6\,\text{s}^{-1}$ 1# $Ca(OH)_2$	Chen [36]
	$E = 117.84 – 134.95\,\text{kJ/mol}, A = 4.04 \times 10^6 – 3.00 \times 10^7\,\text{s}^{-1}$ 2# $Ca(OH)_2$	
	$1.94 \times 10^{12}\, exp\left(\dfrac{-187.88 \times 10^3}{RT}\right) \cdot (1-\dfrac{p}{p_{eq}})^3 \cdot (1-X)\ [X < 0.2]$	Schaube [37]
	$8.96 \times 10^9\, exp\left(\dfrac{-162.62 \times 10^3}{RT}\right) \cdot (1-\dfrac{p}{p_{eq}})^3 \cdot 2(1-X)^{0.5}\ [X > 0.2]$	
	$\dfrac{d\alpha}{dt} = \left(\dfrac{A}{\beta}\right) \cdot exp\left(\dfrac{-E}{RT}\right) \cdot [2(1-\alpha)^{0.5}]$	Long [31]
	$\alpha = 0.2 – 0.8, E = 115 – 140\,\text{kJ/mol}; \beta = 5 – 20\,\text{K/min}, E = 120 – 150\,\text{K/min}$	

In addition to intrinsic properties such as particle size, porosity, and crystallinity, temperature and water vapor pressure critically govern the thermodynamics, kinetics, and mechanistic pathways of calcium hydroxide dehydration. Elevated temperatures lower the Gibbs free energy barrier, favoring decomposition. Changes in vapor pressure shift the equilibrium temperature. Higher temperatures enhance atomic mobility, accelerating both the interfacial reaction, characterized by bond breaking and the diffusion of H_2O through the CaO product layer. The Arrhenius equation quantifies this relationship, with activation energies ranging from 80 to 160 kJ/mol, depending on the rate-limiting step, either nucleation or diffusion. Excessive temperatures cause the sintering of CaO grains, reduce porosity, trap H_2O, and ultimately slow diffusion, leading to incomplete dehydration [38]. Elevated water vapor pressure inhibits the dehydration of $Ca(OH)_2$ by shifting the reaction equilibrium toward rehydration, thereby requiring higher temperatures to sustain the forward reaction rate. Industrial calcination processes typically operate under a vacuum or an inert gas atmosphere to reduce the partial pressure of water vapor and improve dehydration efficiency. Gradients in vapor pressure between the reaction interface and the bulk environment govern the transport of H_2O. At the nanoscale, water molecules adsorbed onto CaO surfaces form transient hydroxyl groups, which modify surface reactivity and influence intermediate reaction pathways [39]. In non-isothermal studies, a compensation effect between temperature and vapor pressure was observed. Lower vapor pressure allowed reactions to occur at lower temperatures. However, excessively rapid heating caused local vapor accumulation. For instance, in the case of CaO, the sharp increase in local vapor pressure induced the formation of micro-fractures within the material. These micro-fractures not only damaged the structural integrity but also altered the diffusion kinetics, thereby affecting the overall reaction rate and the results of thermal analysis [40]. Samms et al. [41] and Halstead et al. [42] employed the Van't Hoff equation $\ln P = -\dfrac{\Delta H}{RT} + C$

to investigate the relationship between pressure P and absolute temperature T, presenting the results as a linear plot of $\ln P$ versus $\frac{1}{T}$, as shown in Figure 3. Schaube et al. [37] predicted the equilibrium temperature of the reaction to be 505 °C at a partial pressure of 1 bar water vapor, which was verified by DSC (differential scanning calorimetry) tests.
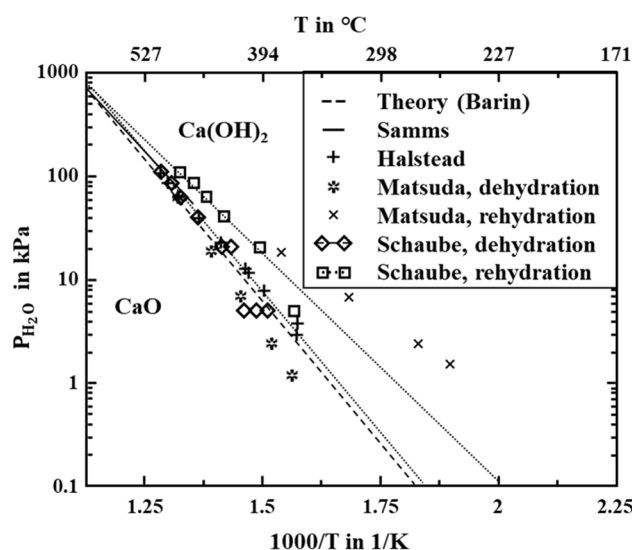

Figure 3. Equilibrium pressure of water vapor versus reaction equilibrium temperature, modified from Ref. [37].

2.2. Hydration Reaction

The hydration process of CaO with H_2O (g) constitutes a gas-solid reaction. The reaction steps are clearly illustrated in Figure 4. The hydration reaction of CaO with H_2O(g) proceeds as a gas-solid reaction involving multiple coupled steps. Initially, external diffusion occurs as water vapor (H_2O) migrates from the bulk gas phase to the external surface of calcium oxide (CaO) particles, driven by concentration gradients and convective/diffusive transport. Subsequently, some water vapor reacts with the particle surface, while the remainder undergoes internal diffusion, transporting through the porous network of the CaO particle via Knudsen or molecular diffusion, depending on pore size and gas pressure. A surface reaction follows, where H_2O(g) chemisorbs at active sites on the CaO surface and reacts to form $Ca(OH)_2$, creating a localized product layer. This product layer then develops, acting as an internal diffusion barrier for reactants, with kinetics limited by solid-state diffusion resistance and interfacial reaction rates. Finally, structural evolution transpires as the progressive growth of the $Ca(OH)_2$ layer induces morphological and textural changes in the particle, modifying porosity, surface area, and diffusion pathways. These simultaneous steps, characterized by mutual influences and constraints, exemplify a multiscale, multi-physical/chemical step-coupled system.

Prior research demonstrates that the full transformation of CaO into $Ca(OH)_2$ transpires within the temperature spectrum of 70 to 420 °C [43]. Lin et al. [44] later confirmed that CaO achieved full hydration under elevated pressure (about 3.8 MPa) at temperatures reaching about 750 °C. The hydration kinetics of CaO were governed by a sophisticated interplay of inherent material characteristics and external environmental factors, with recent experimental advancements yielding profound mechanistic insights. Although elevated temperatures accelerated reaction rates by diminishing activation barriers, excessive heat provoked the sintering of CaO grains, diminishing porosity and entrapping H_2O within the particle core [45]. Conversely, elevated humidity favored the equilibrium shift toward $Ca(OH)_2$ formation yet potentially hindered diffusion by saturating pore channels. Controlled humidity gradients, implemented through fluidized bed reactors, enhanced hydration efficiency by harmonizing interfacial reactivity with vapor transport [8].

Table 3 delineates a spectrum of reaction kinetic models governing the hydration of CaO. Such insights inform the development of CaO-based materials tailored for applications necessitating adjustable hydration rates, including thermochemical energy storage and CO_2 sorbents, where reaction reversibility and cyclability prove paramount.
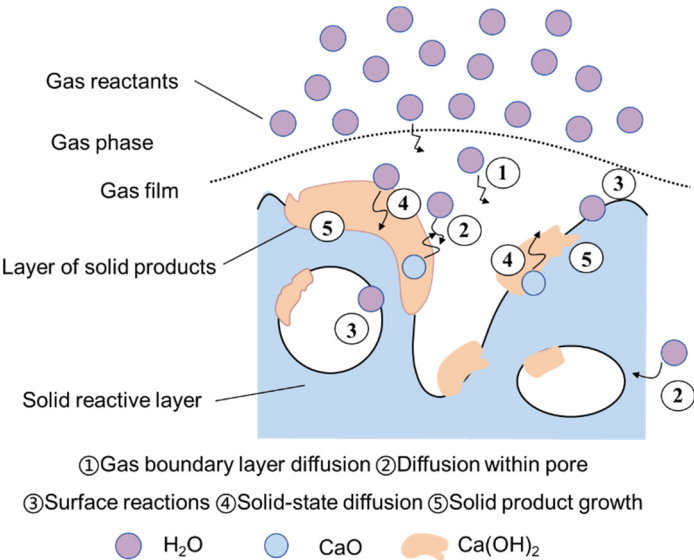
Figure 4. Schematical diagram of hydration of CaO, modified from Ref. [23].

Table 3. Kinetic modelling of CaO hydration reactions.

Method	Reaction Kinetics Modeling	References
High-pressure thermogravimetric	$R = \dfrac{1}{dp^{0.11}} \times 0.0069 exp[-8400/(RT)] \times \left(P_{H_2O} - p_{H_2O}^*\right)^2$	Lin [44]
	$\dfrac{dXHy}{dt} = KHy(T) \cdot \left(v_{H_2O} - v_{eq}\right)f(XHy)$	Criado [11]
Thermal Gravimetric Analyzer	$\dfrac{dx}{dt} = 13945 \times exp\left(\dfrac{-89.486 \times 10^3}{RT}\right) \cdot (\dfrac{p}{p_{eq}} - 1)^{0.83} \cdot 3(1-X) \; [T_{eq} - T \geq 50K]$	Schaube [37]
	$\dfrac{dx}{dt} = 1.00 \times 10^{-34} \, exp\left(\dfrac{53.33 \times 10^3}{T}\right) \cdot (\dfrac{p}{10^5})^6 \cdot (1-X) \; [T_{eq} - T < 50K]$	
	$Rx = 0.1 \; or \; 0.5 = \dfrac{dx}{dt(1-x)}\bigg|_{X=0.1 \, or \, 0.5}$	Lin [46]
	$E = 1.69$ kJ/mol, $A = 5.43 \times 10^{-2}$ s^{-1} (Calcined Ca(OH)$_2$) $E = 1.76$ kJ/mol, $A = 5.74 \times 10^{-3}$ s^{-1} (Sintered Ca(OH)$_2$)	Garcia [47]
Vacuum pump steam mass flowmeter	$ahy = \dfrac{56mH_2O}{18mH_2O} \times 100\%$	Yan [12]

3. Heat and Mass Transfer Characteristics

3.1. Thermal Conductivity

Thermal conductivity exerts a direct influence on the rate of heat dissipation; enhanced thermal conductivity can augment the efficiency of heat exchange and minimize energy loss. However, the inherently low thermal conductivity of Ca(OH)$_2$/CaO materials significantly impairs the efficiency of energy storage. A straightforward method to enhance the thermal conductivity of Ca(OH)$_2$ is by compressing the powder. Ogura et al. [48] experimentally determined that the thermal conductivity of compacted Ca(OH)$_2$ powders ranged from 0.4 to 0.55 W/(m·K) in a fixed-bed reactor, a value approximately four times greater than that of uncompacted Ca(OH)$_2$ powders. In the operation of an indirect reactor, the heat produced by the exothermic hydration reaction must traverse the porous reactant bed to reach the heat exchanger surface, which is in contact with the heat transfer fluid. This process is heavily reliant on the thermal conductivity of the bed, which is directly correlated with the bulk density, typically ranging from 0.5 to 1.5 g/cm^3 for CaO/Ca(OH)$_2$ systems [49,50]. Increasing bulk density enhances thermal conductivity yet simultaneously reduces bed permeability, thereby hindering the diffusion of reacting gases, such as water vapor, to the internal surfaces of the particles. Over compaction can result in the formation of localized barriers to gas transport, causing incomplete reactions and the development of thermal gradients [51].

To balance the competing demands of thermal conductivity and permeability in the bed, a uniform particle distribution within the reactor is crucial. Optimized packing configurations, achieved through graded particle size distributions or mechanical stirring techniques, improve bed homogeneity, thereby balancing thermal conductivity and

gas effective diffusivity [50,52,53]. Yan et al. [29] optimized the calcium-based fixed-bed energy storage reactor by incorporating internal heating tubes. As the particle size within the bed increased from 5 μm to 30 μm, the reaction time gradually decreased and eventually stabilized. The increase in particle size improved the bed's permeability and reduced internal pressure, thereby shortening the reaction time. Risthaus et al. [53] proposed the mechanically fluidized bed, where the radial temperature distribution within the bed remains uniform during the hydration and dehydration reactions of $CaO/Ca(OH)_2$. Under conditions where the effects of rotational speed, pressure, and mass are minimal, the effective heat transfer coefficient during CaO heating is 156 ± 16 W/m^2·K, while the effective heat transfer coefficient during dehydration is 243 ± 52 W/m^2·K, as shown in Figure 5.
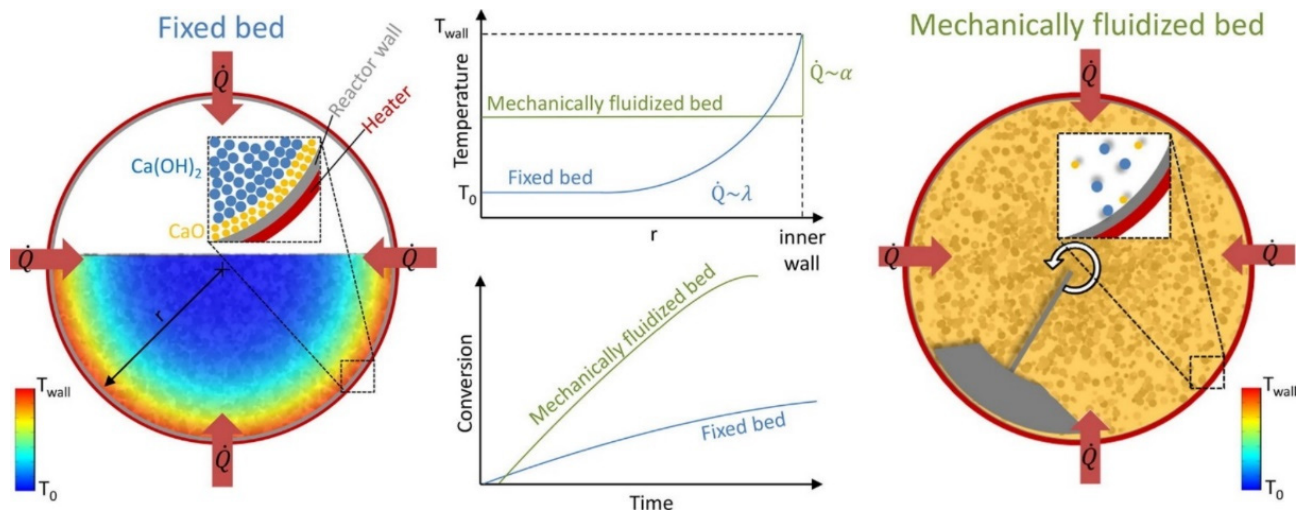

Figure 5. Comparison of temperature distribution and material conversion rate in calcium-based fixed bed and mechanically fluidized bed, modified from Ref. [53].

However, the agglomeration phenomenon that arises during the reaction process within particles such as calcium hydroxide can cause the continuous growth of clustered aggregates throughout the material cycling process. These agglomerates impair both the heat and mass transfer efficiency of the entire system [21]. As the reactions occur within the reactor, its structural and operational characteristics exert a significant influence on the mass and heat transfer performance during thermochemical energy storage. Owing to the generally low thermal conductivity of current reactor beds, heat transfer within the bed emerges as a critical factor. In fixed-bed reactors, internal heat transfer performance is typically inadequate. Moreover, when cyclic processes are conducted in a fixed-bed configuration, agglomerates tend to form after several cycles, resulting in the development of preferential flow channels within the reaction bed. This leads to issues such as uneven distribution of reactant gases [14].

3.2. Flowability

The flowability of calcium hydroxide powder is a pivotal parameter in thermochemical energy storage and industrial applications such as cement hydration and carbon capture, where agglomeration during cyclic operation significantly impairs heat and mass transfer efficiency as well as overall cyclability. This agglomeration stems from strong interparticle cohesive forces, which undermine reactor performance by inducing uneven thermal gradients and limiting the accessibility of reactants. Recent studies have concentrated on mitigating cohesion-induced agglomeration through the use of nanoparticle additives, surface modification strategies, and hybrid material engineering, with the goal of enhancing powder mobility while preserving or improving reaction kinetics. To overcome strong interparticle cohesive forces, nanoparticle coatings have been investigated as spacers that reduce direct contact between particles, thereby mitigating cohesion and improving powder flowability. Roßkopf et al. [54] showed that adding 2% by mass silica nanoparticles to the $CaO/Ca(OH)_2$ cycle effectively prevents particle agglomeration, mitigates the channeling effect, and promotes uniform flow through the reaction bed, thereby enhancing the overall reaction performance of thermochemical energy storage, as shown in Figure 6. The encapsulation of $Ca(OH)_2$ particles with nano-SiO_2 enhances fluidity, preventing agglomeration during cycling and maintaining bed porosity. However, a significant drawback is the parasitic reaction between SiO_2 and $Ca(OH)_2$ at elevated temperatures, which leads to the formation of calcium silicate, thereby reducing the system's cyclic conversion efficiency [55].
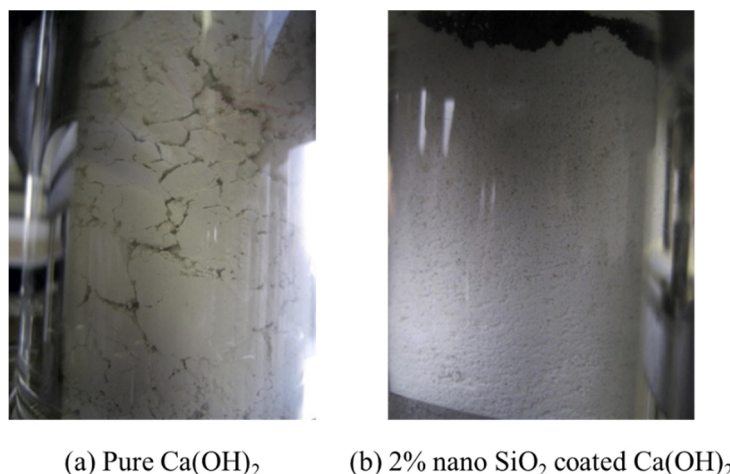
(a) Pure Ca(OH)$_2$ (b) 2% nano SiO$_2$ coated Ca(OH)$_2$

Figure 6. Powder bed, (**a**) pure Ca(OH)$_2$ and (**b**) with addition of two percent of SiO$_2$ nanoparticles at ambient temperature, modified from Ref. [54].

Compound materials based on sodium silicate as the binder for fine CaO/Ca(OH)$_2$ particles have been developed for use in fluidized or fixed beds [56]. Compared to natural calcium-based precursor particles, these materials exhibit superior mechanical properties. However, after several hundred hydration/dehydration cycles, a decline in mechanical performance is observed, primarily due to the anisotropic expansion during the growth process of Ca(OH)$_2$. Bian et al. [57] employed the wet mixing method to prepare SiO$_2$-coated CaO particles using limestone and silica sol as raw materials. It was found that the SiO$_2$-coated CaO particles exhibited better structural stability and heat release performance. After 10 thermal storage cycles, the expansion rate and wear rate of the SiO$_2$-coated CaO particles were reduced by 45.4% and 48.5%, respectively, compared to the uncoated particles, while the volumetric energy density increased by 33.2%. In addition to coating CaO/Ca(OH)$_2$ with nanoparticles and modifying pure particles, incorporating larger particles into the CaO/Ca(OH)$_2$ bed can also enhance its flowability. Pardo et al. [49] incorporated fluidizable particles, specifically 81.4 μm Al$_2$O$_3$, into pure Ca(OH)$_2$ particles at a mass ratio of 7:3. This mixture exhibited excellent flow stability in a fluidized bed and maintained good heat storage and release capacity after 50 cycles. Mejia et al. [58] conducted 20 heat storage and release cycles on Al$_2$O$_3$-coated Ca(OH)$_2$ particles and Ca(OH)$_2$/CaCO$_3$ composite materials. Both samples exhibited improved mechanical strength and structural integrity, preventing crack formation, fracturing, and agglomeration of Ca(OH)$_2$ particles.

4. Cyclic Stability of Ca(OH)$_2$/CaO

4.1. Agglomerate and Sintering

Various forces, such as van der Waals forces, hydrogen bonding, and electrostatic forces between powder particles, are the root cause of agglomeration formation [59]. Due to the large surface area and high surface energy of Ca(OH)$_2$ particles, the agglomeration phenomenon will be triggered between the powder particles due to mutual attraction. The agglomeration and sintering of CaO particles during high-temperature cycles, such as in calcium looping for CO$_2$ capture or thermochemical energy storage, pose significant challenges by reducing reactivity, porosity, and cycling stability. Sintering, induced by atomic diffusion and surface energy minimization at temperatures above 800 °C, causes irreversible particle coalescence and pore collapse. Meanwhile, agglomeration results from interparticle van der Waals, capillary, or electrostatic forces, intensified by repeated hydration/dehydration or carbonation/calcination cycles [60]. Agglomeration forms secondary particles, increasing particle size and impairing the cyclic stability of CaO/Ca(OH)$_2$-based thermochemical energy storage systems, resulting in reduced conversion rates and lower energy storage efficiency.

For calcium-based materials, using finer particles as reactants exacerbates agglomeration and adhesion, hindering full contact and heat transfer between particles. Conversely, employing larger particles to mitigate agglomeration and enhance mobility impedes reaction gas diffusion into the particles, leading to incomplete reactions. Dai et al. [61] investigated the cyclic stability of the dehydration/hydration process of Ca(OH)$_2$. After 20 consecutive cycles, significant agglomeration was observed in the reactants. They hypothesized that the accumulation of agglomerates reduces the permeability of the reaction bed. The accumulation of agglomerates in the reaction bed not only increases the pressure drop but also hinders effective contact between water vapor and calcium oxide during hydration, significantly reducing heat transfer performance. Agglomeration can be mitigated by reducing particle-to-particle attraction through

two approaches: converting powders into larger particles, which is challenging due to volume changes during reactions, or coating particle surfaces with additives to increase surface roughness and decrease interparticle attraction.

Bian et al. [62] investigated the exothermic performance of CaO particles in different states within a CaO/Ca(OH)$_2$-based thermochemical energy storage system. In the first cycle, the average exothermic temperature of static CaO was significantly higher than that of the fluidized state, as the static state's convective heat transfer is less effective, and the carrier gas in the fluidized state removes substantial heat. However, the exothermic capacity of static CaO declines with increasing cycles, primarily due to pronounced agglomeration in the static state. In contrast, the fluidized state exhibits superior cycling stability, as shown in Figure 7.
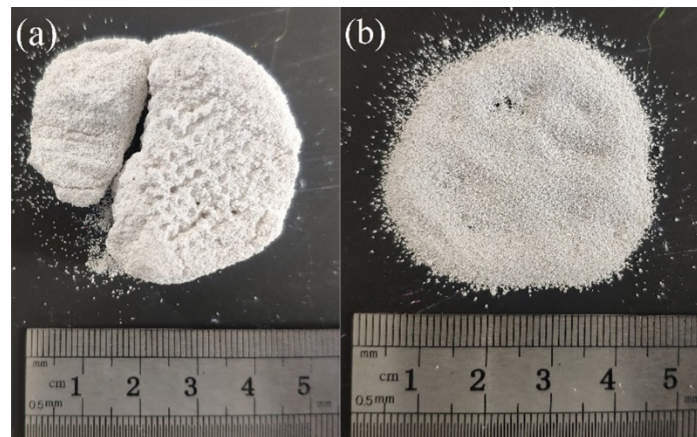

Figure 7. Images of CaO experienced 5 heat storage cycles: (**a**) CaO under static state, (**b**) CaO under fluidization state, modified from Ref. [62].

Investigating particle agglomeration behavior at the molecular level offers valuable insights into the relationship between microscopic reaction mechanisms and agglomeration dynamics. As shown in Figure 8, Xu et al. [20] employed molecular dynamics simulations to study the aggregation process between two nanoscale CaO and Ca(OH)$_2$ particles. The results demonstrated that, in the presence of water, Ca(OH)$_2$ particles exhibited a significantly faster aggregation rate compared to CaO particles. Furthermore, the incorporation of nanoscale SiO$_2$ as a barrier material in CaO/Ca(OH)$_2$-based thermochemical energy storage systems effectively reduced the agglomeration rate during thermochemical reactions. Wang et al. [63] further investigated the molecular dynamics mechanisms underlying particle agglomeration in SiO$_2$-doped CaO/Ca(OH)$_2$ systems. Their analysis revealed the intrinsic mechanism by which SiO$_2$ suppresses hydration-induced agglomeration of CaO. Specifically, upon SiO$_2$ incorporation, particle agglomeration was primarily governed by external potential energy, while the absolute rate of internal potential energy change remained relatively low. This led to a reduction in the driving force for agglomeration, resulting in lower aggregation degrees and enhanced structural stability, thereby reducing the propensity for particle agglomeration.
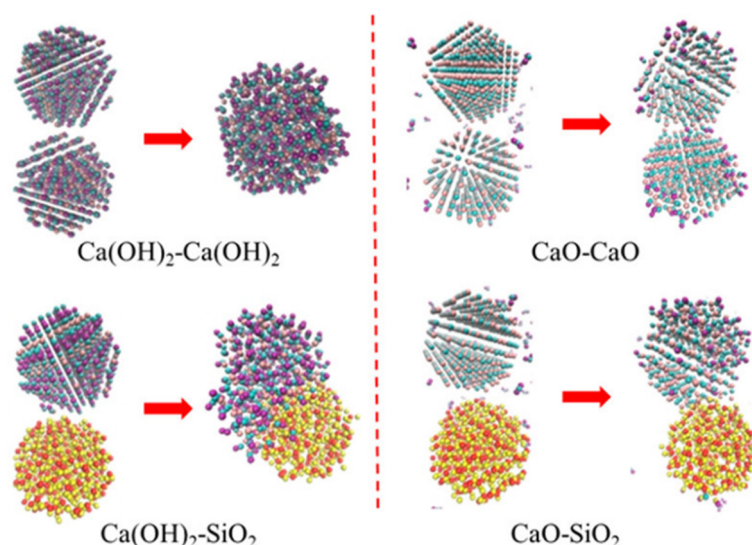

Figure 8. Snapshots from molecular dynamics simulations illustrating the reactive behavior of two Ca(OH)$_2$ particles, two CaO particles, and Ca(OH)$_2$ and CaO particles under SiO$_2$-doped conditions modified from Ref. [20].

4.2. Sintering Kinetics of Calcium-Based Materials

Sintering refers to the agglomeration of calcium oxide particles induced by elevated temperatures during repeated dehydration and hydration cycles. The study of sintering kinetics on the surface of particle clusters, combined with the reaction process, can elucidate the complex interaction mechanisms, structural evolution, and dehydration/hydration dynamics in $CaO/Ca(OH)_2$ thermochemical energy storage systems.

The sintering model utilizes a standard two-sphere configuration to simulate neck formation between adjacent particles through two distinct mechanistic pathways: surface-mediated processes involving surface diffusion and evaporation-condensation, and bulk transport mechanisms including plastic flow, grain boundary diffusion, and volume diffusion, as shown in Figure 9. Two-sphere sintering model sintering model captures the essential physics of particle coalescence while maintaining computational tractability for analyzing sintering behavior in particulate systems [64].
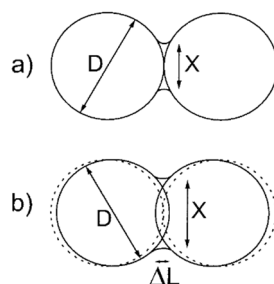

Figure 9. Different sintering mechanisms, (**a**) surface area diffusion mechanism and (**b**) volume diffusion mechanism, modified from Ref. [64].

Wu et al. [65] investigated the temperature-dependent microstructural evolution between two calcium oxide particles using Gaussian and LAMMPS simulations. The results indicated that initial sintering occurred within the temperature range of 700–900 K, during which the increased temperature effectively mitigated the rise in mass transfer resistance caused by sintering. However, when the temperature exceeded 900 K, complete sintering was observed, and further temperature elevation could no longer compensate for the increased mass transfer resistance. Recent studies indicate that the sintering kinetics of CaO are driven by its low Tammann temperature, facilitating surface diffusion at moderate temperatures (600–900 °C). Advanced in situ characterization techniques, including synchrotron X-ray nano tomography and environmental transmission electron microscopy (ETEM), demonstrate that sintering begins with neck formation between adjacent particles, followed by grain boundary migration and densification, ultimately collapsing the mesoporous structure critical for gas-solid reactions [66]. Gu et al. [25] investigated the sintering kinetics during the non-isothermal dehydration of $Ca(OH)_2$, deriving reaction rate equations for both analytical-grade and industrial-grade $Ca(OH)_2$. Their findings confirmed that sintering is more pronounced at lower heating rates, explaining the enhanced sintering behavior in certain fixed-bed reactors during the heat storage and release processes of $CaO/Ca(OH)_2$ systems, attributed to low heat transfer rates.

Despite significant progress, achieving an optimal balance between sintering resistance, cost-effectiveness, and scalability remains a major challenge. Techniques such as atomic layer deposition (ALD) and the use of nanostructured materials often incur high production costs, while excessive doping levels may compromise the CO_2 capture capacity of CaO. Recent innovations have introduced hybrid strategies, including the development of CaO–perovskite composites that synergistically enhance both thermal stability and catalytic performance [67], as well as MOF-templated CaO structures exhibiting ultrahigh porosity to retard densification. Looking forward, emerging approaches such as machine learning–guided screening of anti-sintering additives and thermally responsive self-healing coatings offer promising directions, as emphasized in perspective by Zhang et al. [68]. In summary, although particle agglomeration and sintering continue to pose significant barriers, advances in materials engineering, nanotechnology, and computational design are progressively enabling the development of robust, high-performance CaO-based systems.

5. Efficiency Improvement of Calcium-Based Energy Storage Systems

Transitioning from laboratory-scale investigations to industrial implementation, $Ca(OH)_2/CaO$ thermochemical energy storage systems require enhanced cyclic stability and optimized energy storage efficiency to meet practical application demands. Current research efforts reveal that prolonged cycling induces progressive deterioration in chemical reactivity and structural integrity of calcium-based composites. These technical limitations stem from inherent

material characteristics, including but not limited to suboptimal thermal conductivity, particle agglomeration phenomena, thermal sintering tendencies, and heterogeneous heat release profiles. To address these challenges, dual optimization strategies focusing on both reactor engineering and material modification have emerged as promising solutions. From a structural perspective, reactor redesign could enhance heat/mass transfer efficiency, while material-level interventions through nano structuring techniques or composite formulation may mitigate degradation mechanisms and improve reaction kinetics.

5.1. Calcium Matrix Composites Modification

The $CaO/Ca(OH)_2$ gas-solid reaction system represents a highly promising thermochemical energy storage platform for calcium-based materials, with dual applicability in concentrated solar power (CSP) generation and carbon dioxide capture [69]. Despite its potential, widespread implementation faces persistent material-level challenges, including particle agglomeration, thermal sintering, suboptimal thermal conductivity, and heterogeneous heat release profiles. To mitigate these limitations, researchers have strategically engineered calcium-based composite materials through nano structuring, doping, or hybrid matrix integration, aiming to enhance reaction kinetics and stabilize cyclic performance.

Wang et al. [70] improved the overall energy storage efficiency of the $Ca(OH)_2/CaO$ system by adding KNO_3, and the results showed that the addition of 10 wt% of KNO_3 could reduce the reaction temperature to 428.49 °C, which led to a greatly accelerated reaction speed and almost no loss of energy storage density. KNO_3 itself has good stability, and it does not negatively affect the reaction stability of the $Ca(OH)_2/CaO$ thermochemical energy storage system. Yan et al. [71] modified $Ca(OH)_2$ particles by adding Li. Comparing the effect of Li addition on the dehydration process of $Ca(OH)_2$, it was found that the dehydration rate of $Ca(OH)_2$ could be increased without affecting the energy storage capacity. Kariya et al. [72] obtained calcium matrix composites by using expanded graphite and $Ca(OH)_2$ preparation, which improved the heat and mass transfer efficiency inside the particles. Thermodynamic analysis showed that doping Li or Mg on thermochemical energy storage materials had little effect on the enthalpy of generation. Some research results showed that the enthalpy of generation of CaO when doped with Li is very small, although not negative [22]. This shows that only a small amount of energy is needed to replace CaO with Li doping in the $CaO/Ca(OH)_2$ energy storage system to improve the energy storage capacity.

A critical limitation of the $CaO/Ca(OH)_2$ thermochemical energy storage system lies in its inherent mechanical instability. Specifically, CaO particles derived from natural limestone calcination demonstrate pronounced susceptibility to particle attrition and fracture during repeated hydration/dehydration cycles. This structural degradation becomes particularly problematic given the system's operational requirements: prolonged exposure to high-pressure steam or oxidative atmospheres during thermal cycling necessitates robust mechanical integrity to prevent gas entrapment and mitigate pressure gradient fluctuations across the reactor bed. To address these challenges, prior studies have explored material reinforcement strategies, predominantly focusing on binder-assisted palletization or dopant-enhanced stabilization of calcium-based matrices.

Surface engineering innovations, particularly ALD of Al_2O_3 or TiO_2, have demonstrated significant potential for passivating CaO surfaces and mitigating particle degradation mechanisms during thermochemical cycling. Kim et al. [73] achieved a 2-nm Al_2O_3 coating on CaO via ALD. The Al_2O_3 coating effectively mitigates sintering while stabilizing the porous microstructure through the formation of calcium aluminate ($Ca_3Al_2O_6$), thereby preserving adsorption capacity and maintaining excellent cyclic stability. Zhang et al. [74] synthesized CaO-based thermal energy storage materials using bamboo fiber as a bio-template and Al_2O_3 doping. The templated material increased energy storage density by 24,131.44 kJ/kg over 50 cycles compared to limestone, with the CaO-based material doped with 5 wt.% Al_2O_3 and 0.5 g bamboo fiber showing 2.7 times higher energy storage density and a carbonation conversion of 0.75 mol/mol after 10 cycles.

Calcium matrix composites are synthesized through strategic doping with inert materials to address the intrinsic limitations of raw calcium-based compounds, including particle agglomeration, thermal sintering, and poor thermal conductivity. These dopants introduce controlled lattice strain that creates diffusion barriers at particle boundaries, effectively inhibiting sintering behavior. However, while laboratory-scale results demonstrate improved stability, the practical implementation of these composites remains constrained by economic viability and scalability challenges for industrial applications.

5.2. Reactor Design and Optimization

Currently, research on CaO/Ca(OH)$_2$ thermochemical energy storage systems remains predominantly at the laboratory scale. To facilitate the transition from fundamental research to industrial implementation, systematic evaluation of reactor configurations and optimization of energy storage efficiency are critically needed. The reactor design for calcium-based thermochemical energy storage systems has attracted significant research attention, particularly considering the unique requirements of the CaO/Ca(OH)$_2$ dehydration/hydration cycle—a classic gas-solid reversible reaction system. Among available reactor types, fixed-bed and fluidized-bed configurations have emerged as the most widely studied options for such gas-solid reaction processes.

Fixed-bed reactors have been extensively utilized in industrial applications owing to their operational simplicity, making them a natural focus for thermochemical energy storage research. These systems typically employ two primary configurations: direct-contact and indirect-contact designs, each offering distinct heat and mass transfer characteristics for gas-solid reactions. Schaube et al. [14] evaluated the cyclic performance of a direct-contact fixed-bed reactor for Ca(OH)$_2$ dehydration/hydration, demonstrating that 60 g samples maintained stable total conversion and consistent reaction rates throughout 25 consecutive thermal cycles. Regarding fixed-bed reactor configurations, indirect-contact systems face significant application limitations due to their inherently low thermal conductivity. In contrast, direct-contact designs offer superior heat transfer characteristics, presenting a more viable alternative for thermochemical energy storage applications [75]. Funayama et al. [76] employed cylindrical Ca(OH)$_2$ particles (Ø1.9 mm × L2–10 mm length, $\rho = 1.2$ g/cm^3, total mass = 59.6 g) in thermogravimetric cycling tests, as shown in Figure 10. The particles maintained consistent reaction kinetics over 17 consecutive dehydration/hydration cycles, demonstrating excellent cyclic stability and confirming the technical feasibility of fixed-bed reactors for CaO/Ca(OH)$_2$ thermochemical energy storage systems.
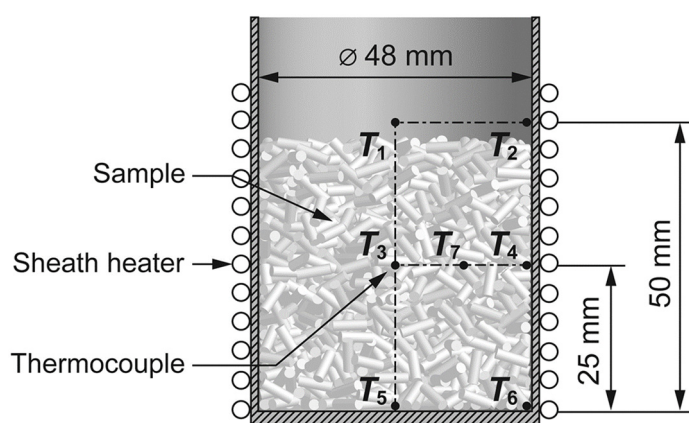

Figure 10. Sectional view of the cylindrical packed bed reactor, modified from Ref. [76].

To address the inherent limitations of fixed-bed reactors—including excessive heat transfer area requirements, suboptimal heat/mass transfer efficiency, narrow operational ranges, and elevated capital costs—researchers have focused on reactor design innovations to enhance the energy storage capacity of calcium-based thermochemical systems. Recent advances have demonstrated the potential of fluidized-bed reactors for calcium-based thermochemical energy storage, with numerous studies highlighting their superior performance characteristics compared to conventional fixed-bed configurations. Pardo et al. [49] demonstrated the feasibility of a CaO/Ca(OH)$_2$ thermochemical energy storage system in a fluidized-bed reactor, conducting 50 consecutive dehydration (480 °C) and hydration (350 °C) cycles using a 1.93 kg mixed sample composed of 30 wt% Ca(OH)$_2$ and 70 wt% Al$_2$O$_3$ as a fluidizing medium. Criado et al. [77] developed an innovative single-cycle fluidized bed reactor system for CaO/Ca(OH)$_2$ thermochemical energy storage, specifically designed for continuous hydration/dehydration operations. The reactor configuration, when integrated with a large-capacity solid storage silo, achieved remarkable performance characteristics, including a maximum thermal output of 100 MW$_t$, an energy storage density of 260 kWh/m^3, and net processing efficiency of 63% at hydration flow rates between 390–460 m^3/h. Wang et al. enhanced intra-reactor transport processes through innovative structural modifications, incorporating highly permeable and thermally conductive porous channels within the conventional fluidized bed design. These engineered channels serve dual functions by facilitating efficient steam evacuation to drive the CaO/Ca(OH)$_2$ dehydration equilibrium while simultaneously enhancing localized heat transfer to accelerate reaction kinetics. This integrated approach effectively addresses both mass and heat transfer limitations characteristic of standard fluidized bed reactors, demonstrating significant potential for optimizing thermochemical energy storage systems. The

permeable channels promote reactant flow dynamics, whereas their thermal conductivity properties improve energy distribution, collectively boosting overall reactor performance. To improve the transport processes within the reactor, Wang et al. [78] proposed structural optimization by incorporating porous channels featuring both high permeability and thermal conductivity into the conventional fluidized bed reactor design. These modified channels function dually: their high permeability facilitates efficient steam discharge, thereby promoting the $CaO/Ca(OH)_2$ dehydration reaction, while their enhanced thermal conductivity improves local heat transfer rates, consequently accelerating the overall dehydration process. Uchino et al. [79] developed a model for an unsteady fluidized bed reactor based on the conversion of $Ca(OH)_2$ to CaO. When nitrogen was used as the fluidizing gas, bed temperature fluctuations increased with greater heat supply fluctuations, with heat supply fluctuations having a more significant impact than bed temperature variations. In contrast, when water vapor was used as the fluidizing gas, heat supply fluctuations had minimal effect on bed temperature stability. This is primarily because the dehydration rate under water vapor conditions is more temperature-dependent than under nitrogen conditions. Thus, nitrogen is a preferable fluidizing gas for optimizing energy storage efficiency during the dehydration process. Wang et al. [80] investigated the heat transfer coefficient in the $CaO/Ca(OH)_2$ heat storage and release process within a fluidized bed reactor equipped with internal heating wires. The study evaluated heat transfer performance under various operating conditions, including steam pressure and reaction temperature. A bed-to-heat transfer surface model was applied and compared with experimental results, yielding a relative error of approximately 7.14%. The structure and heat transfer performance of the fluidized bed are illustrated in Figure 11.
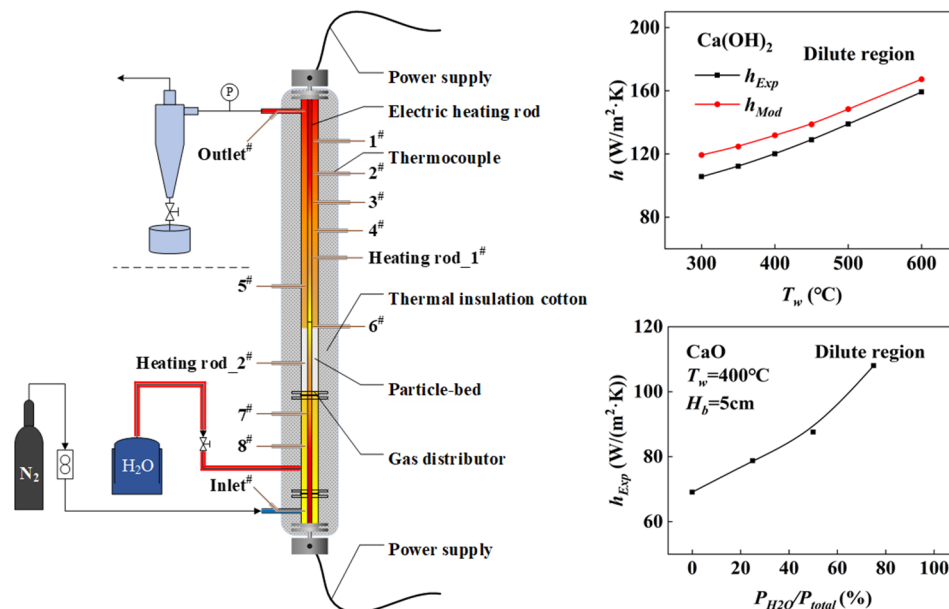

Figure 11. Schematic of fluidized bed heating apparatus and heat transfer performance in the $CaO/Ca(OH)_2$ heat storage and release process, modified from Ref. [80].

In addition to the common fixed-bed and fluidized-bed reactors, in order to overcome the problems of poor mobility and low thermal conductivity, many researchers have proposed the design concept of moving-bed reactors. Schmidt et al. [81] developed a novel moving-bed reactor with a capacity of 10 kW/100 kWh, utilizing 270 kg of $Ca(OH)_2$, for a $CaO/Ca(OH)_2$-based thermochemical energy storage system. Mejia et al. [82] developed a novel countercurrent moving-bed reactor for a $CaO/Ca(OH)_2$-based thermochemical energy storage system, shown in Figure 12, where unreacted cold material enters from the top, and hot air is introduced from the bottom. The energy storage material flows downward through the pipe under gravity. Heat transfer is facilitated by a heat transfer fluid flowing on one side of a heat exchanger, guided by folding plates that promote rapid air circulation, ensuring a high heat transfer coefficient between the airflow and the pipe surface.
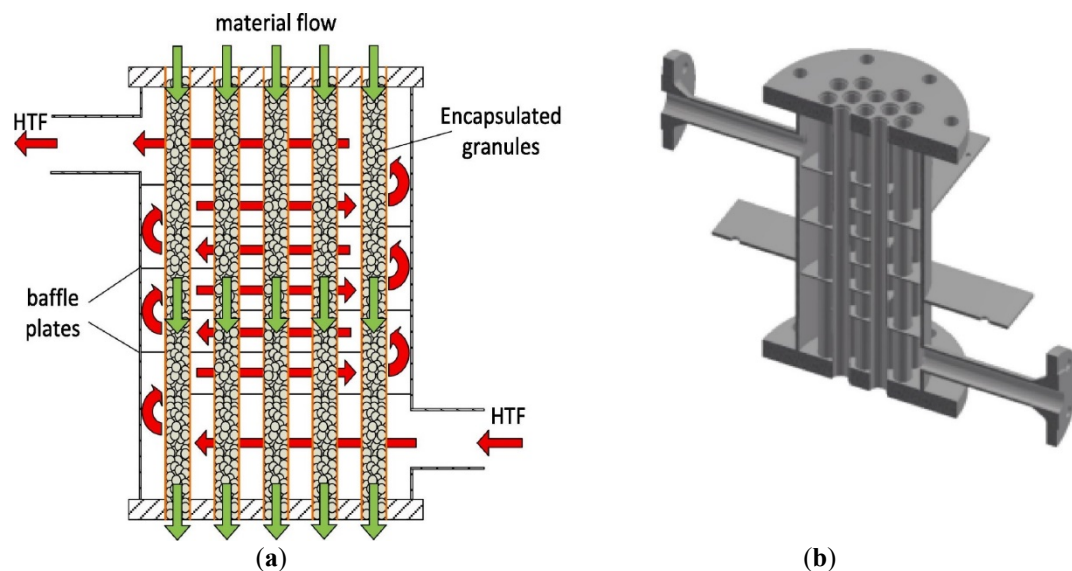
Figure 12. Moving bed reactor designed by Mejia et al. [82]. (**a**) Schematic representation of the flow of the HTF on the shell side (red arrows) and the storage material in the tubes of the reactor (green arrows). (**b**) 3D image of the tube-bundle reactor, modified from Ref. [82].

From a reactor design perspective, enhancing the energy storage efficiency of thermochemical systems based on modified calcium-based materials requires addressing several key challenges. These include optimizing the reactor wall temperature and inlet/outlet pressures, controlling the particle size and physical state of the reactive materials, improving internal heat and mass transfer, and mitigating particle agglomeration and sintering during reactions. Numerous researchers have proposed innovative reactor designs and process improvements, each offering distinct advantages and limitations. However, current research remains largely in the experimental phase, and the transition from laboratory-scale studies to industrial-scale applications of calcium-based thermochemical energy storage reactors still demands extensive exploration and development.

6. Conclusions and Outlook

The global transition to renewable energy highlights the need for effective energy storage solutions, with thermochemical energy storage systems like $CaO/Ca(OH)_2$ being particularly promising due to their high energy density, cost-effectiveness, and compatibility with renewable sources. However, several challenges hinder its industrial use, including cycling stability issues caused by sintering and particle agglomeration, incomplete understanding of reaction kinetics under various conditions, trade-offs between heat transfer and energy storage capacity, and the limited exploration of thermodynamic effects when modifying materials with dopants.

To address these challenges and advance the $CaO/Ca(OH)_2$ TCES system, future research should focus on: (1) developing strategies to prevent sintering, such as nanoengineering and surface modification, while ensuring reversibility in hydration/dehydration cycles; (2) creating multiscale kinetic models to understand better reaction mechanisms and the impact of temperature, pressure, and dopants; (3) designing composite materials (e.g., hybrid structures with graphene or metal foams) to improve heat transfer without sacrificing energy storage capacity; (4) investigating the thermodynamic effects of dopants to optimize energy storage, sintering resistance, and cost; (5) exploring integrated systems that combine TCES with CO_2 capture or waste-heat recovery to enhance sustainability; and (6) testing these systems at pilot scale to assess long-term performance, economic viability, and compatibility with existing infrastructure.

Author Contributions

Conceptualization, Z.S. and F.L.; Methodology, Z.S. and D.W.; Software, J.W.; Validation, Y.G. (Yongchuan Gao), Y.D. and Q.L.; Formal Analysis, Z.S.; Investigation, J.W. and Y.G. (Yishi Gu); Resources, H.L.; Data Curation, D.Y. and Z.D.; Writing—Original Draft Preparation, J.W.; Writing—Review & Editing, J.W. and Z.S.; Visualization, Q.L.; Supervision, H.L.; Project Administration, H.L.; Funding Acquisition, F.L.

Ethics Statement

The study was "Not applicable" for studies not involving humans or animals.

Informed Consent Statement

Informed consent was obtained from all subjects involved in the study.

Data Availability Statement

Data will be made available on request.

Funding

Declaration of Competing Interest

The authors declare that they have no known competing financial interests or personal relationships that could have appeared to influence the work reported in this paper.

References

1. Gbenou T, Fopah-Lele A, Wang K. Recent Status and Prospects on Thermochemical Heat Storage Processes and Applications. *Entropy* **2021**, *23*, 953. doi:10.3390/e23080953.
2. Saleh HM, Hassan AI. The challenges of sustainable energy transition: A focus on renewable energy. *Appl. Chem. Eng.* **2024**, *7*, 2084. doi:10.59429/ace.v7i2.2084.
3. Wang K, Yan T, Li RK, Pan WG. A review for Ca(OH)$_2$/CaO thermochemical energy storage systems. *J. Energy Storage* **2022**, *50*, 104612. doi:10.1016/j.est.2022.104612.
4. Beyne W, De Paepe M, Degroote J. A sizing model for a tube in tube sensible thermal energy storage heat exchanger with solid storage material. *J. Energy Storage* **2025**, *105*, 114622. doi:10.1016/j.est.2024.114622.
5. Liu K, Wu C, Gan H, Liu C, Zhao J. Latent heat thermal energy storage: Theory and practice in performance enhancement based on heat pipes. *J. Energy Storage* **2024**, *97*, 112844. doi:10.1016/j.est.2024.112844.
6. Zhao J, Korba D, Mishra A, Klausner J, Randhir K, AuYeung N, et al. Particle-based high-temperature thermochemical energy storage reactors. *Prog. Energy Combust. Sci.* **2024**, *102*, 101143. doi:10.1016/j.pecs.2024.101143.
7. Chen X, Zhang Z, Qi C, Ling X, Peng H. State of the art on the high-temperature thermochemical energy storage systems. *Energy Convers. Manag.* **2018**, *177*, 792–815. doi:10.1016/j.enconman.2018.10.011.
8. Rougé S, Criado YA, Soriano O, Abanades JC. Continuous CaO/Ca(OH)$_2$ Fluidized Bed Reactor for Energy Storage: First Experimental Results and Reactor Model Validation. *Ind. Eng. Chem. Res.* **2017**, *56*, 844–852. doi:10.1021/acs.iecr.6b04105.
9. Dean CC, Blamey J, Florin NH, Al-Jeboori MJ, Fennell PS. The calcium looping cycle for CO$_2$ capture from power generation, cement manufacture and hydrogen production. *Chem. Eng. Res. Des.* **2011**, *89*, 836–855. doi:10.1016/j.cherd.2010.10.013.
10. Carro A, Chacartegui R, Ortiz C, Becerra JA. Analysis of a thermochemical energy storage system based on the reversible Ca(OH)$_2$/CaO reaction. *Energy* **2022**, *261*, 125064. doi:10.1016/j.energy.2022.125064.
11. Criado YA, Alonso M, Abanades JC. Kinetics of the CaO/Ca(OH)$_2$ Hydration/Dehydration Reaction for Thermochemical Energy Storage Applications. *Ind. Eng. Chem. Res.* **2014**, *53*, 12594–12601. doi:10.1021/ie404246p.
12. Yan J, Zhao CY. Experimental study of CaO/Ca(OH)$_2$ in a fixed-bed reactor for thermochemical heat storage. *Appl. Energy* **2016**, *175*, 277–284. doi:10.1016/j.apenergy.2016.05.038.
13. Rosemary JK, Bauerle GL, Springer TH. Solar Energy Storage Using Reversible Hydration-Dehydration of CaO-Ca(OH)$_2$. *J. Energy* **1979**, *3*, 321–322. doi:10.2514/3.62440.
14. Schaube F, Kohzer A, Schütz J, Wörner A, Müller-Steinhagen H. De- and rehydration of Ca(OH)$_2$ in a reactor with direct heat transfer for thermo-chemical heat storage. Part A: Experimental results. *Chem. Eng. Res. Des.* **2013**, *91*, 856–864. doi:10.1016/j.cherd.2012.09.020.
15. Bai S, Sun J, Zhou Z, Bu C, Chen X, Yang Y, et al. Structurally improved, TiO$_2$-incorporated, CaO-based pellets for thermochemical energy storage in concentrated solar power plants. *Sol. Energy Mater. Sol. Cells* **2021**, *226*, 111076. doi:10.1016/j.solmat.2021.111076.
16. Carrillo AJ, González-Aguilar J, Romero M, Coronado JM. Solar Energy on Demand: A Review on High Temperature Thermochemical Heat Storage Systems and Materials. *Chem. Rev.* **2019**, *119*, 4777–4816. doi:10.1021/acs.chemrev.8b00315.
17. Yuan Y, Li Y, Zhao J. Development on Thermochemical Energy Storage Based on CaO-Based Materials: A Review.

Sustainability **2018**, *10*, 2660. doi:10.3390/su10082660.

18. Boning R. Review on thermal properties and reaction kinetics of Ca(OH)$_2$/CaO thermochemical energy storage materials. *Electr. Mater. Appl.* **2024**, *1*, e12007. doi:10.1049/ema3.12007.

19. Huang C, Xu M, Li X, Huai X. Remarkable low-temperature dehydration kinetics of rare-earth-ion-doped Ca(OH)$_2$ for thermochemical energy storage. *Chem. Eng. J.* **2023**, *478*, 147475. doi:10.1016/j.cej.2023.147475.

20. Xu M, Huai X, Cai J. Agglomeration Behavior of Calcium Hydroxide/Calcium Oxide as Thermochemical Heat Storage Material: A Reactive Molecular Dynamics Study. *J. Phys. Chem. C* **2017**, *121*, 3025–3033. doi:10.1021/acs.jpcc.6b08615.

21. Wang K, Zhang CM, Liu BC, Yang L, Min CH, Rao ZH. Agglomeration inhibition mechanism of SiO$_2$ in the Ca(OH)$_2$/CaO thermochemical heat storage process: A reactive molecular dynamics study. *Chem. Eng. J.* **2024**, *480*, 148118. doi:10.1016/j.cej.2023.148118.

22. Yan J, Zhao CY. First-principle study of CaO/Ca(OH)$_2$ thermochemical energy storage system by Li or Mg cation doping. *Chem. Eng. J.* **2014**, *117*, 293–300. doi:10.1016/j.ces.2014.07.007.

23. Zhenshan L, Ningsheng C. Rate equation theory for gas-solid reaction kinetics. *J. Tsinghua Univ. (Sci. Technol.)* **2022**, *62*, 704–721.

24. Cai J, Li Z. First principles-based kinetic analysis of Ca(OH)$_2$ dehydration in thermochemical energy storage system. *J. Energy Storage* **2024**, *97*, 112759. doi:10.1016/j.est.2024.112759.

25. Gu Y, Cheng Y, Shen Z, Lv F, Wan D, Gao Y, et al. Study on non-isothermal reaction and sintering kinetics of Ca(OH)$_2$ particle cluster dehydration with temperature distribution modification. *Chem. Eng. J.* **2024**, *488*, 151015. doi:10.1016/j.cej.2024.151015.

26. Karayiannis NC, Mavrantzas VG, Theodorou DN. Diffusion of small molecules in disordered media: Study of the effect of kinetic and spatial heterogeneities. *Chem. Eng. Sci.* **2001**, *56*, 2789–2801.

27. Zhou J, Liu C, Lu J. Influence of Ca(OH)$_2$ modification on the pore structure and properties of porous glass-ceramics stepwise sintered from granite sludge. *Constr. Build. Mater.* **2024**, *429*, 136436. doi:10.1016/j.conbuildmat.2024.136436.

28. Luo JW, Chen L, Wang M, Xia Y, Tao W. Particle-scale study of coupled physicochemical processes in Ca(OH)$_2$ dehydration using the lattice Boltzmann method. *Energy* **2022**, *250*, 123835. doi:10.1016/j.energy.2022.123835.

29. Yan J, Jiang L, Zhao C. Numerical Simulation of the Ca(OH)$_2$/CaO Thermochemical Heat Storage Process in an Internal Heating Fixed-Bed Reactor. *Sustainability* **2023**, *15*, 7141. doi:10.3390/su15097141.

30. Wang S, Wu F, Di BB, Yan Y, Tang YC. Intensification Effect of a Multi-Jet Structure on a Multiphase Flow and Desulfurization Process in a Fluidized Bed. *ACS Omega* **2023**, *8*, 5861–5876. doi:10.1021/acsomega.2c07658.

31. Long XF, Dai L, Lou B, Wu J. The kinetics research of thermochemical energy storage system Ca(OH)$_2$/CaO. *Int. J. Energy Res.* **2017**, *41*, 1004–1013. doi:10.1002/er.3688.

32. Hu R, Shi Q. *Thermal Analysis Kinetics*; Science Press: Beijing, China, 2001.

33. Mikhail RS, Brunauer S, Copeland LE. Kinetics of the thermal decomposition of calcium hydroxide. *J. Colloid Interface Sci.* **1966**, *21*, 394–404. doi:10.1016/0095-8522(66)90005-5.

34. Dutta S, Shirai T. Experimental investigation on a fast and exothermic solid-liquid reaction system. *Chem. Eng. Sci.* **1980**, *35*, 209–216. doi:10.1016/00092509(80)80089-3.

35. Chaix-Pluchery O, Pannetier J, Bouillot J, Niepce JC. Structural prereactional transformations in Ca(OH)$_2$. *J. Solid State Chem.* **1987**, *67*, 225–234. doi:10.1016/0022-4596(87)90358-6.

36. Chen D, Gao X, Dollimore D. The application of non-isothermal methods of kinetic analysis to the decomposition of calcium hydroxide. *Thermochim. Acta* **1993**, *215*, 65–82. doi:10.1016/0040-6031(93)80082-L.

37. Schaube F, Koch L, Wörner A, Müller-Steinhagen H. A thermodynamic and kinetic study of the de- and rehydration of Ca(OH)$_2$ at high H$_2$O partial pressures for thermo-chemical heat storage. *Thermochim. Acta* **2012**, *538*, 9–20. doi:10.1016/j.tca.2012.03.003.

38. Yan J, Zhao CY, Xia BQ, Wang T. The effect of dehydration temperatures on the performance of the CaO/Ca(OH)$_2$ thermochemical heat storage system. *Energy* **2019**, *186*, 115837. doi:10.1016/j.energy.2019.07.167.

39. Fujimori Y, Zhao X, Shao X, Levchenko SV, Nilius N, Sterrer M, et al. Interaction of Water with the CaO(001) Surface. *J. Phys. Chem. C* **2016**, *120*, 5565–5576. doi:10.1021/acs.jpcc.6b00433.

40. Schmidt M, Gutierrez A, Linder M. Thermochemical energy storage with CaO/Ca(OH)$_2$—Experimental investigation of the thermal capability at low vapor pressures in a lab scale reactor. *Appl. Energy* **2017**, *188*, 672–681. doi:10.1016/j.apenergy.2016.11.023.

41. Samms JAC, Evans BE. Thermal dissociation of Ca(OH)$_2$ at elevated pressures. *J. Appl. Chem.* **1968**, *18*, 5–8. doi:10.1002/jctb.5010180102.

42. Halstead PE, Moore AE. The thermal dissociation of calcium hydroxide. *J. Chem. Soc. (Resumed)* **1957**, 3873–3875. doi:10.1039/JR9570003873.

43. Serris E, Favergeon L, Pijolat M, Soustelle M, Nortier P, Gärtner RS, et al. Study of the hydration of CaO powder by gas–solid reaction. *Cem. Concr. Res.* **2011**, *41*, 1078–1084. doi:10.1016/j.cemconres.2011.06.014.

44. Lin S, Harada M, Suzuki Y, Hatano H. CaO Hydration Rate at High Temperature (~1023 K). *Energy Fuels* **2006**, *20*, 903–

908. doi:10.1021/ef050257o.

45. Kuwata K, Esaki T, Iwase D, Ito H, Li S, Yang X, et al. Long-Term Durability and Reactivation of Thermochemical Heat Storage Driven by the CaO/Ca(OH)$_2$; Reversible Reaction. *J. Mater. Sci. Chem. Eng.* **2017**, *05*, 23–32. doi:10.4236/msce.2017.511003.

46. Lin S, Wang Y, Suzuki Y. High-Temperature CaO Hydration/Ca(OH)$_2$ Decomposition over a Multitude of Cycles. *Energy Fuels* **2009**, *23*, 2855–2861. doi:10.1021/ef801088x.

47. García YC, Martínez I, Grasa G. Determination of the hydration and carbonation kinetics of CaO for low-temperature applications. *Chem. Eng. Sci.* **2024**, *295*, 120146. doi:10.1016/j.ces.2024.120146.

48. Ogura H, Miyazaki M, Matsuda H, Hasatani M. Experimental Study on Heat Transfer Enhancement of the Solid Reactant Particle Bed in a Chemical Heat Pump Using Ca(OH)$_2$/CaO Reaction. *KAGAKU KOGAKU RONBUNSHU Jpn.* **1991**, *17*, 916–923. doi:10.1252/kakoronbunshu.17.916.

49. Pardo P, Anxionnaz-Minvielle Z, Rougé S, Cognet P, Cabassud M. Ca(OH)$_2$/CaO reversible reaction in a fluidized bed reactor for thermochemical heat storage. *Sol. Energy* **2014**, *107*, 605–616. doi:10.1016/j.solener.2014.06.010.

50. Gollsch M, Linder M. Influence of structural changes on gas transport properties of a cycled CaO/Ca(OH)$_2$ powder bulk for thermochemical energy storage. *J. Energy Storage* **2023**, *73*, 108790. doi:10.1016/j.est.2023.108790.

51. Schmidt M, Linder M. Power generation based on the Ca(OH)$_2$/CaO thermochemical storage system—Experimental investigation of discharge operation modes in lab scale and corresponding conceptual process design. *Appl. Energy* **2017**, *203*, 594–607. doi:10.1016/j.apenergy.2017.06.063.

52. Mejia AC, Afflerbach S, Linder M, Schmidt M. Development of a Moving Bed Reactor for Thermochemical Heat Storage Based on Granulated Ca(OH)$_2$. *Processes* **2022**, *10*, 1680. doi:10.3390/pr10091680.

53. Risthaus K, Linder M, Schmidt M. Experimental investigation of a novel mechanically fluidized bed reactor for thermochemical energy storage with calcium hydroxide/calcium oxide. *Appl. Energy* **2022**, *315*, 118976. doi:10.1016/j.apenergy.2022.118976.

54. Roßkopf C, Haas M, Faik A, Linder M, Wörner A. Improving powder bed properties for thermochemical storage by adding nanoparticles. *Energy Convers. Manag.* **2014**, *86*, 93–98. doi:10.1016/j.enconman.2014.05.017.

55. Roßkopf C, Afflerbach S, Schmidt M, Görtz B, Kowald T, Linder M, et al. Investigations of nano coated calcium hydroxide cycled in a thermochemical heat storage. *Energy Convers. Manag.* **2015**, *97*, 94–102. doi:10.1016/j.enconman.2015.03.034.

56. Criado YA, Alonso M, Abanades JC. Enhancement of a CaO/Ca(OH)$_2$ based material for thermochemical energy storage. *Sol. Energy* **2016**, *135*, 800–809. doi:10.1016/j.solener.2016.06.056.

57. Bian Z, Li Y, Fang Y, Ren Y, Zhao J. Thermochemical heat storage performance and structural stability of SiO2-coated CaO particles under fluidization in CaO/Ca(OH)$_2$ cycles. *J. Energy Storage* **2024**, *85*, 111102. doi:10.1016/j.est.2024.111102.

58. Mejia AC, Afflerbach S, Linder M, Schmidt M. Real-time visualization and experimental analysis of stabilized Ca(OH)$_2$ granules for thermal energy storage. *Energy Convers. Manag. X* **2024**, *23*, 100656. doi:10.1016/j.ecmx.2024.100656.

59. Zheng QJ, Yang RY, Zeng QH, Zhu HP, Dong KJ, Yu AB. Interparticle forces and their effects in particulate systems. *Powder Technol.* **2024**, *436*, 119445. doi:10.1016/j.powtec.2024.119445.

60. Yuan Y, Li Y, Duan L, Liu H, Zhao J, Wang Z. CaO/Ca(OH)$_2$ thermochemical heat storage of carbide slag from calcium looping cycles for CO$_2$ capture. *Energy Convers. Manag.* **2018**, *174*, 8–19. doi:10.1016/j.enconman.2018.08.021.

61. Dai L, Long XF, Lou B, Wu J. Thermal cycling stability of thermochemical energy storage system Ca(OH)$_2$/CaO. *Appl. Therm. Eng.* **2018**, *133*, 261–268. doi:10.1016/j.applthermaleng.2018.01.059.

62. Bian Z, Li Y, Zhang C, Zhao J, Wang T, Lei W. Heat release performance and evolution of CaO particles under fluidization for CaO/Ca(OH)$_2$ thermochemical heat storage. *Process Saf. Environ. Prot.* **2021**, *155*, 166–176. doi:10.1016/j.psep.2021.09.019.

63. Wang K, Liu BC, Zhang CM, Min CH, Rao ZH. A reactive molecular dynamics study of the sintering and inhibition mechanism of Ca(OH)$_2$/CaO hydroxide heat storage materials during the exothermic process. *Chem. Eng. J.* **2025**, *505*, 158862. doi:10.1016/j.cej.2024.158862.

64. Pérez-Maqueda LA, Criado JM, Real C. Kinetics of the Initial Stage of Sintering from Shrinkage Data: Simultaneous Determination of Activation Energy and Kinetic Model from a Single Nonisothermal Experiment. *J. Am. Ceram. Soc.* **2002**, *85*, 763–768. doi:10.1111/j.1151-2916.2002.tb00169.x.

65. Wu W, Wang T, Wang D, Jin B. Mechanism of HCl removal by CaO based on Gaussian and LAMMPS simulation. *J. Southeast Univ. (Nat. Sci. Ed.)* **2020**, *50*, 1–10.

66. Mirghiasi Z, Bakhtiari F, Darezereshki E, Esmaeilzadeh E. Preparation and characterization of CaO nanoparticles from Ca(OH)$_2$ by direct thermal decomposition method. *J. Ind. Eng. Chem.* **2014**, *20*, 113–117. doi:10.1016/j.jiec.2013.04.018.

67. Yue W, Yu Z, Ma X, Liu H, Li W. Enhanced stability of Ni-CaO catalysts by perovskite-type stabilizer in biomass pyrolysis for hydrogen production. *J. Anal. Appl. Pyrolysis* **2023**, *174*, 106130. doi:10.1016/j.jaap.2023.106130.

68. Zhang WW, Wei ZY, Zhang LY, Xing YZ, Zhang Q. Low-thermal-conductivity thermal barrier coatings with a multi-scale pore design and sintering resistance following thermal exposure. *Rare Met.* **2020**, *39*, 352–367. doi:10.1007/s12598-020-01393-6.

69. Zhang C, Li Y, Yuan Y, Wang Z, Wang T, Lei W. Simultaneous CO_2 capture and heat storage by a Ca/Mg-based composite in coupling calcium looping and $CaO/Ca(OH)_2$ cycles using air as a heat transfer fluid. *React. Chem. Eng.* **2021**, *6*, 100–111. doi:10.1039/D0RE00351D.

70. Wang T, Zhao CY, Yan J. Investigation on the $Ca(OH)_2/CaO$ thermochemical energy storage system with potassium nitrate addition. *Sol. Energy Mater. Sol. Cells* **2020**, *215*, 110646. doi:10.1016/j.solmat.2020.110646.

71. Yan J, Zhao CY. Thermodynamic and kinetic study of the dehydration process of $CaO/Ca(OH)_2$ thermochemical heat storage system with Li doping. *Chem. Eng. Sci.* **2015**, *138*, 86–92. doi:10.1016/j.ces.2015.07.053.

72. Kariya J, Ryu J, Kato Y. Reaction Performance of Calcium Hydroxide and Expanded Graphite Composites for Chemical Heat Storage Applications. *ISIJ Int.* **2015**, *55*, 457–463. doi:10.2355/isijinternational.55.457.

73. Kim SM, Armutlulu A, Kierzkowska AM, Hosseini D, Donat F, Müller C. Development of an effective bi-functional Ni–CaO catalyst-sorbent for the sorption-enhanced water gas shift reaction through structural optimization and the controlled deposition of a stabilizer by atomic layer deposition. *Sustain. Energy Fuels* **2020**, *4*, 713–729. doi:10.1039/C9SE00619B.

74. Zhang H, Ma X, Huang X, Li F, Li J, Hu X, et al. Biotemplating of Al_2O_3-Doped, CaO-Based Material from Bamboo Fiber for Efficient Solar Energy Storage. *Processes* **2023**, *11*, 460. doi:10.3390/pr11020460.

75. Schaube F, Wörner A, Tamme R. High Temperature Thermochemical Heat Storage for Concentrated Solar Power Using Gas–Solid Reactions. *J. Sol. Energy Eng.* **2011**, *133*, 031006. doi:10.1115/1.4004245.

76. Funayama S, Takasu H, Zamengo M, Kariya J, Kim ST, Kato Y. Performance of thermochemical energy storage of a packed bed of calcium hydroxide pellets. *Energy Storage* **2019**, *1*, e40. doi:10.1002/est2.40.

77. Criado YA, Alonso M, Abanades JC, Anxionnaz-Minvielle Z. Conceptual process design of a $CaO/Ca(OH)_2$ thermochemical energy storage system using fluidized bed reactors. *Appl. Therm. Eng.* **2014**, *73*, 1087–1094. doi:10.1016/j.applthermaleng.2014.08.065.

78. Wang M, Chen L, He P, Tao W-Q. Numerical study and enhancement of $Ca(OH)_2/CaO$ dehydration process with porous channels embedded in reactors. *Energy* **2019**, *181*, 417–428. doi:10.1016/j.energy.2019.05.184.

79. Uchino T, Fushimi C. Fluidized bed reactor for thermochemical heat storage using $Ca(OH)_2/CaO$ to absorb the fluctuations of electric power supplied by variable renewable energy sources: A dynamic model. *Chem. Eng. J.* **2021**, *419*, 129571. doi:10.1016/j.cej.2021.129571.

80. Wang J, Gu Y, Yuan D, Shen Z, Xu J, Liu H. Heat transfer characteristics of $CaO/Ca(OH)_2$ particle fluidization for thermochemical energy storage. *Particuology* **2025**, *102*, 41–52. doi:10.1016/j.partic.2025.04.005.

81. Schmidt M, Gollsch M, Giger F, Grün M, Linder M. Development of a moving bed pilot plant for thermochemical energy storage with $CaO/Ca(OH)_2$. *AIP Conf. Proc.* **2016**, *1734*, 050041. doi:10.1063/1.4949139.

82. Mejia AC, Afflerbach S, Linder M, Schmidt M. Experimental analysis of encapsulated $CaO/Ca(OH)_2$ granules as thermochemical storage in a novel moving bed reactor. *Appl. Therm. Eng.* **2020**, *169*, 114961. doi:10.1016/j.applthermaleng.2020.114961.